Supporting Information

Template-assisted alloying of atom-precise silver nanoclusters: a new approach to generate cluster functionality

Sourav Biswas, [a] ‡ *Anish Kumar Das,* [a] ‡ *Surya Sekhar Manna,* [b] *Biswarup Pathak,* [b] *Sukhendu Mandal* [a] *

[a]School of Chemistry, Indian Institute of Science Education and Research Thiruvananthapuram, Kerala 695551, India. Email: sukhendu@iisertvm.ac.in

[b] Department of Chemistry, Indian Institute of Technology Indore, Madhya Pradesh 453552, India.

‡ Both SB and AKD contributed equally.

Table of contents

Experimental

Materials

Silver nitrate ($AgNO_3$), silver trifluoroacetate (CF_3COOAg), tert butylthiol (HS^tBu), tetra-n-butylammonium hexafluorophosphate, tetrakis(acetonitrile)copper(I) tetrafluoroborate ($Cu(CH_3CN)_4BF_4$) were procured from Sigma-Aldrich. HPLC grade solvents- triethylamine (Et_3N), dimethylacetamide (DMA), dimethylformamide (DMF), dichloromethane (DCM), acetonitrile (ACN), ethanol (EtOH) and methanol (MeOH) were purchased from Spectrochem.

X-ray Crystallography Details

Bruker Axs Kappa Apex II SCXRD (single crystal X-ray diffractometer) with CCD detector (MoKα radiation, λ= 0.71073 Å) was used here. The crystal structures were solved by SHELXT 2014 and refined by the full matrix least-squares method using SHELXL 2018 present in the program suite WinGX (version 2014.1).[S1-S3] All non-hydrogen atoms were refined anisotropically and hydrogen atoms were (positioned geometrically) refined isotropically using an olex2.[S4]

Computational Details

All the structures optimizations have done using DFT method in Gaussian 09 software.[S5] The B3LYP functional with Pople's 6-31G* basis set[S6,S7] and LANL2DZ effective core potential (ECP)[S8,S9] were used for the nonmetallic elements (S, F, O, N, C and H) and metal (Ag, Cu), respectively. The TD-DFT has performed for electronic absorption spectra with the scanning of 300 excited state. We have used conductor like polarizable continuum solvent model for all the considered NCs.[S10] The non-covalent interaction (NCI) plot and critical points were performed through the reduced density gradient (RDG) using the quantum theory of atoms in molecules (QTAIM) method implemented in the Multiwfn program (version-3.8).[S11,S12] Besides, the Kohn-Sham orbital analysis has been performed for the understanding of core and ligands orbital contribution in the frontier molecular orbitals using Multiwfn program.[S11]

The projected density of states (PDOS) calculation for the compounds at the bulk level is carried out using Vienna Ab-Initio Simulation Package (VASP) for all the three NCs by using Generalized gradient approximation of Perdew–Burke–Ernzerhof (PBE) functional.[S13,S14] Projector augmented wave (PAW) method has been applied for the consideration of interaction between core and valence electrons.[S14] The energy cut-off of 470 eV has been implemented for

geometry optimization. The ionic relaxations have been carried out using a conjugate gradient algorithm with convergence criteria of 10^{-5} eV/Å for minimum energy and ≤ 0.05 eV/Å for Hellmann-Feynman forces on atoms. Due to the large size of the unit cells of the compounds, the Brillouin zone was sampled at the Gamma point of (1×1×1). For the PDOS calculation, a higher (2×2×2) K-point is used.

Instrumentation

UV-vis spectroscopy was carried out on a UV-3800 SHIMADZU UV−vis/NIR spectrometer. Emission measurements were performed using a Fluorolog-3 spectrofluorimeter from Horiba Jobin Yvon. The relative quantum yield was determined by the best match of the excitation wavelength of a well-known chromophore such as pyrene with the NC and the excitation was fixed at 317 nm. The concentration of the chloroform solutions was fixed by adjusting the absorption 0.05 OD and measured the quantum yield at room temperature. A picosecond time-correlated single-photon counting (TCSPC) system (Horiba Jobin Yvon-IBH) was utilized for the measurement of emission lifetime after excitation with a 340 nm pulsed diode laser. FEI Tecnai G2 F30 S-Twin transmission electron microscope (TEM) 300 KV and FEI Nova NANOSEM 450 (with EDS) were used for the microscopic characterization. X-ray photoelectron spectroscopy (XPS) measurements have been done using the Omicron Nano tech instrument (MgKα radiation at 1253.6 eV). All binding energies were referenced to the neutral C 1*s* peak at 284.8 eV. Cyclic voltammogram (CV) were measured on a CH instrument with a three-electrode system where glassy carbon electrode (GCE) was used as a working electrode, graphite electrode served as a counter electrode and silver wire was used as a reference electrode in DCM with 0.05 M tetra-n-butylammonium hexafluorophosphate salt was added as an electrolyte. We have calibrated against the standard reference electrode (Ag/Ag^+). A Bruker Avance III, 500 MHz, NMR was used. The electrical measurement was done by using a Keithley 6712 electrometer.

ESI-MS measurement

Waters Q-TOF mass spectrometer equipped with a Z-spray source was used for the electrospray ionization (ESI) mass spectrometry measurement with positive mode. **NC 1** crystals were dissolved in DCM (1 mg/mL) and diluted by acetonitrile (1:1). The solution was infused at 20 µL/min for positive mode. The spectrometer was operated in the mass range of m/z 2000–5000 for positive mode.

Instrument parameters	ES+ (positive mode)
Capillary (kV)	2.9000
Sampling Cone	146.0000
Source Temperature (°C)	70
Source Offset	30
Desolvation Temperature (°C)	100
Cone Gas Flow (L/Hr)	153
Desolvation Gas Flow (L/Hr)	214

The **NC 2** was dissolved in DCM (1 mg/mL) and diluted by acetonitrile (1:1). The solution was infused at 25 µL/min for positive mode. The spectrometer was operated in the mass range of m/z 2000–5000 for positive mode.

Instrument parameters	ES+ (positive mode)
Capillary (kV)	2.6000
Sampling Cone	143.0000
Source Temperature (°C)	70
Source Offset	50
Desolvation Temperature (°C)	100
Cone Gas Flow (L/Hr)	142
Desolvation Gas Flow (L/Hr)	292

The **NC 3** was dissolved in DCM (1mg/ml) and diluted by acetonitrile (1:1). The solution was infused at 25 µL/min for positive mode. The spectrometer was operated in the mass range of m/z 2000–5000 for positive mode.

Instrument parameters	ES+ (positive mode)
Capillary (kV)	3.4400
Sampling Cone	117.0000
Source Temperature (°C)	70
Source Offset	39
Desolvation Temperature (°C)	100
Cone Gas Flow (L/Hr)	157.0
Desolvation Gas Flow (L/Hr)	631.0

Table S1. Crystal data and structure refinement parameters of **NC 1**.

Identification code	**NC 1**
CCDC number	2183686
Empirical formula	$C_{68}H_{114}Ag_{20}F_{24}N_4O_{18}S_{11}$
Formula weight	4241.69
Temperature	150 K
Wavelength	0.71073 Å
Crystal system	Monoclinic
Space group	$P2_1/n$
Unit cell dimensions	a = 16.3357(12) Å; b = 16.1055(12) Å, c = 23.5813(17) Å; α = 90°; β = 94.397(10)°; γ = 90°
Volume	6185.9(8) $Å^3$
Z	2
Density	2.277 mg/m^3
Absorption coefficient	3.356 mm^{-1}
F(000)	4052
Crystal size	0.095 × 0.050 × 0.038 mm
Theta range for data collection	2.410 to 28.050°
Limiting indices	-21<=h<=21, -21<=k<=21, -31<=l<=31
Reflections collected	89860
Independent reflections	15437 [R(int) = 0.0959]
Completeness to theta = 25.242°	99.9 %
Refinement method	Full-matrix least-squares on F^2
Data / restraints / parameters	15437 / 42 / 648
Goodness-of-fit on F^2	1.044
Final R indices [I > 2sigma(I)]	R_1 = 0.0717, wR_2 = 0.1881
R indices (all data)	R_1 = 0.1295, wR_2 = 0.2219
Largest diff. peak and hole	3.541 and -3.380 e. $Å^{-3}$

Table S2. Crystal data and structure refinement parameters of **NC 2**.

Identification code	**NC 2**
CCDC number	2183687
Empirical formula	$C_{69}H_{118}Ag_{20}F_{24}N_4O_{24}S_{10}$
Formula weight	4321.67
Temperature	150 K
Wavelength	0.71073 Å
Crystal system	Monoclinic
Space group	$P2_1/c$
Unit cell dimensions	a = 15.4136(17) Å; b = 30.794(3) Å, c = 28.051(3) Å; α = 90°; β = 103.798(2)°; γ = 90°
Volume	12930(2) $Å^3$
Z	4
Density	2.220 mg/m^3
Absorption coefficient	3.201 mm^{-1}
F(000)	8272
Crystal size	0.085 × 0.078 × 0.048 mm
Theta range for data collection	0.998 to 28.416°
Limiting indices	-20<=h<=20, -41<=k<=41, -37<=l<=36
Reflections collected	188717
Independent reflections	32294 [R(int) = 0.1480]
Completeness to theta = 25.242°	100.0 %
Refinement method	Full-matrix least-squares on F^2
Data / restraints / parameters	32294 / 1580 / 1338
Goodness-of-fit on F^2	1.025
Final R indices [I > 2sigma(I)]	R_1 = 0.0938, wR_2 = 0.2318
R indices (all data)	R_1 = 0.2141, wR_2 = 0.2987
Largest diff. peak and hole	4.030 and -1.698 e. $Å^{-3}$

Table S3. Crystal data and structure refinement parameters of **NC 3**.

Identification code	**NC 3**
CCDC number	2183688
Empirical formula	$C_{162}H_{288}Ag_{40}Cu_2F_{48}N_{12}O_{48}S_{23}$
Formula weight	9263.29
Temperature	150 K
Wavelength	0.71073 Å
Crystal system	Monoclinic
Space group	$P2_1/n$
Unit cell dimensions	a = 15.9453(15) Å; b = 18.3040(17) Å, c = 24.394(2) Å; α = 90°; β = 105.548(2)°; γ = 90°
Volume	6859.2(11) $Å^3$
Z	1
Density	2.243 mg/m^3
Absorption coefficient	3.197 mm^{-1}
F(000)	4466
Crystal size	0.040 × 0.037 × 0.028 mm
Theta range for data collection	2.060 to 28.449°
Limiting indices	-21<=h<=21, -24<=k<=24, -32<=l<=32
Reflections collected	115684
Independent reflections	17208 [R(int) = 0.1553]
Completeness to theta = 25.242°	99.9 %
Refinement method	Full-matrix least-squares on F^2
Data / restraints / parameters	17208 / 126 / 797
Goodness-of-fit on F^2	1.027
Final R indices [I > 2sigma(I)]	R_1 = 0.0626, wR_2 = 0.1452
R indices (all data)	R_1 = 0.1504, wR_2 = 0.1831
Largest diff. peak and hole	2.603 and -1.723 e. $Å^{-3}$

Table S4. The obtained radiative, nonradiative rate constants, quantum yield and lifetime of **NC 3**.

Temperature (K)	**Relative quantum yield (ϕ)**	**Lifetime (τ_{av}) (ns)**	**k_r (s^{-1})**	**k_{nr} (s^{-1})**
273	0.25	14	1.78×10^7	5.35×10^7
298	0.21	12	1.75×10^7	6.58×10^7
308	0.11	8	1.37×10^7	11.12×10^7

Table S5. Single-crystal conductivity of each NC.

Crystal Name	**L (cm)**	**W $(cm)^2$**	**Conductance (S)**	**Conductivity ($S.\ cm^{-1}$)**
NC 1	0.0017	0.034	2.32×10^{-7}	1.2×10^{-8}
NC 2	0.0022	0.033	2.57×10^{-7}	1.7×10^{-8}
NC 3	0.003	0.054	1.1×10^{-2}	6.1×10^{-4}

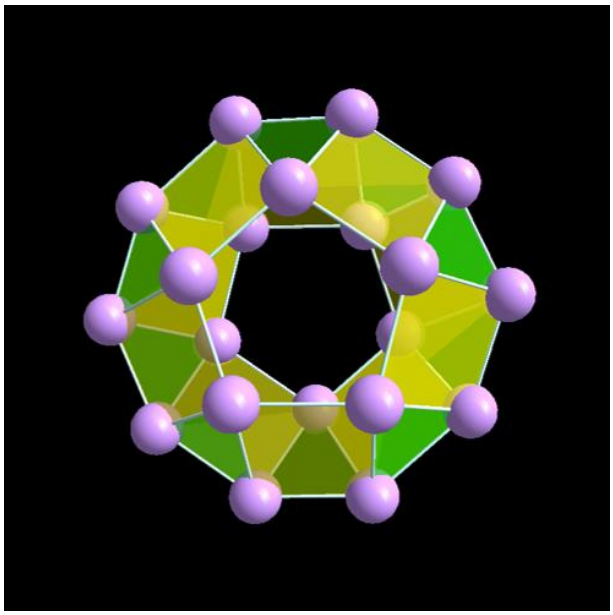

Fig. S1 Doughnut-like Ag_{20} core.

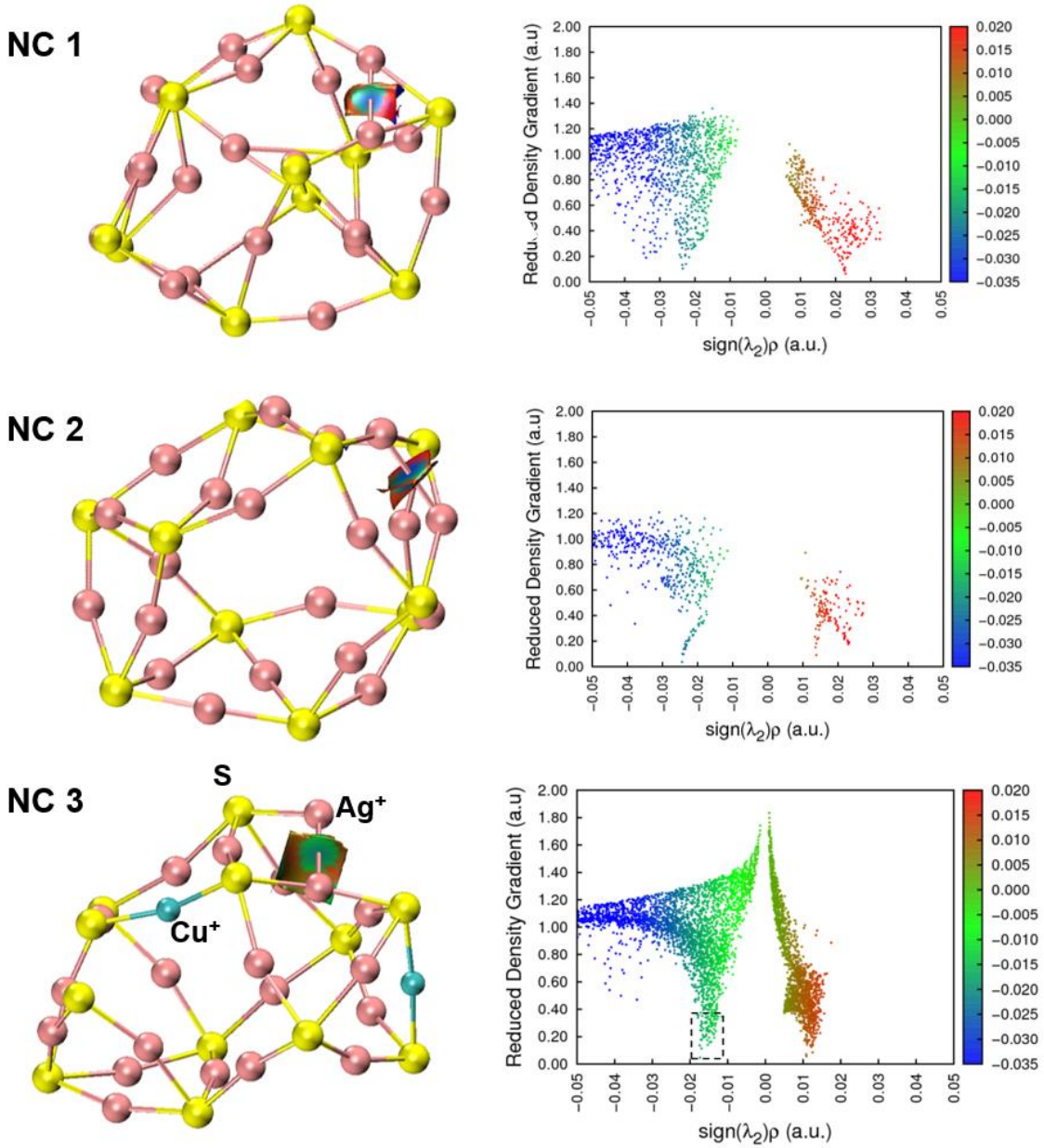

Fig. S2 The Reduced Density Gradient (RDG) isosurface of argentophilic interaction and the associated corresponding scatter plot of (RDG *vs*. sign(λ_2)ρ) of each NC. Where the green color in the plot indicates the presence of nonbonding interaction.

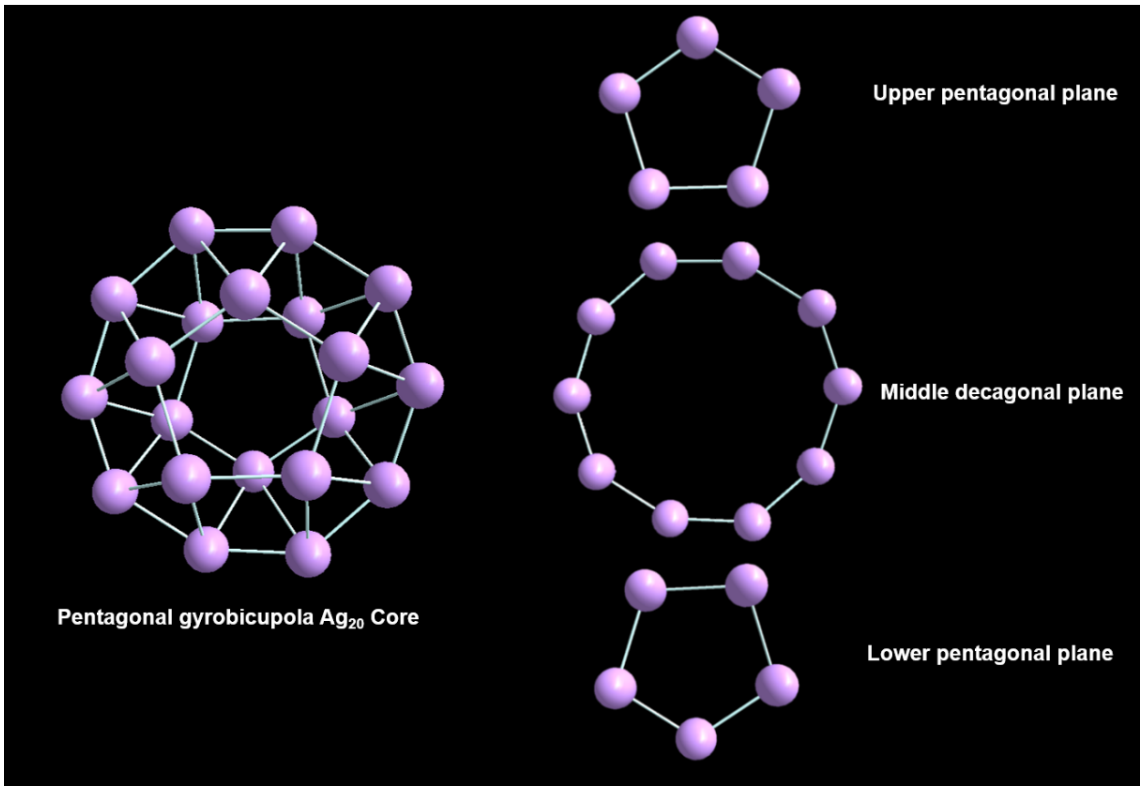

Fig. S3 The three planes of Ag_{20} skeleton.

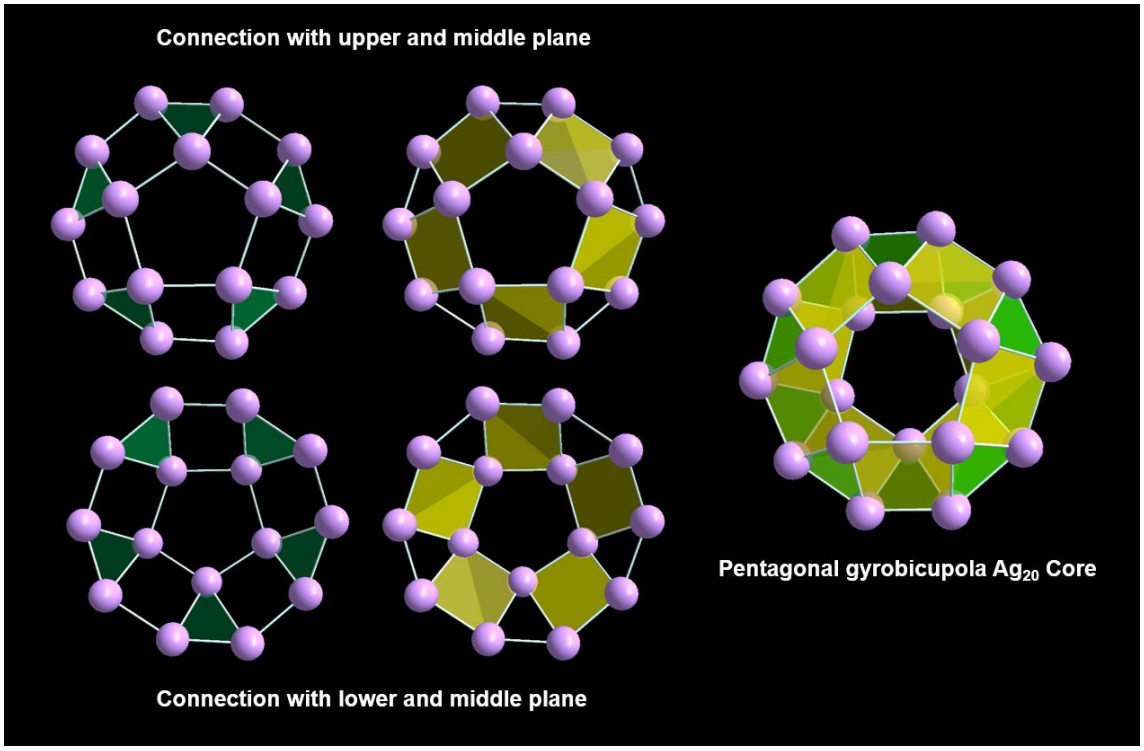

Fig. S4 The middle plane of Ag_{20} core is connected with the other two planes through ten square and ten triangular facets.

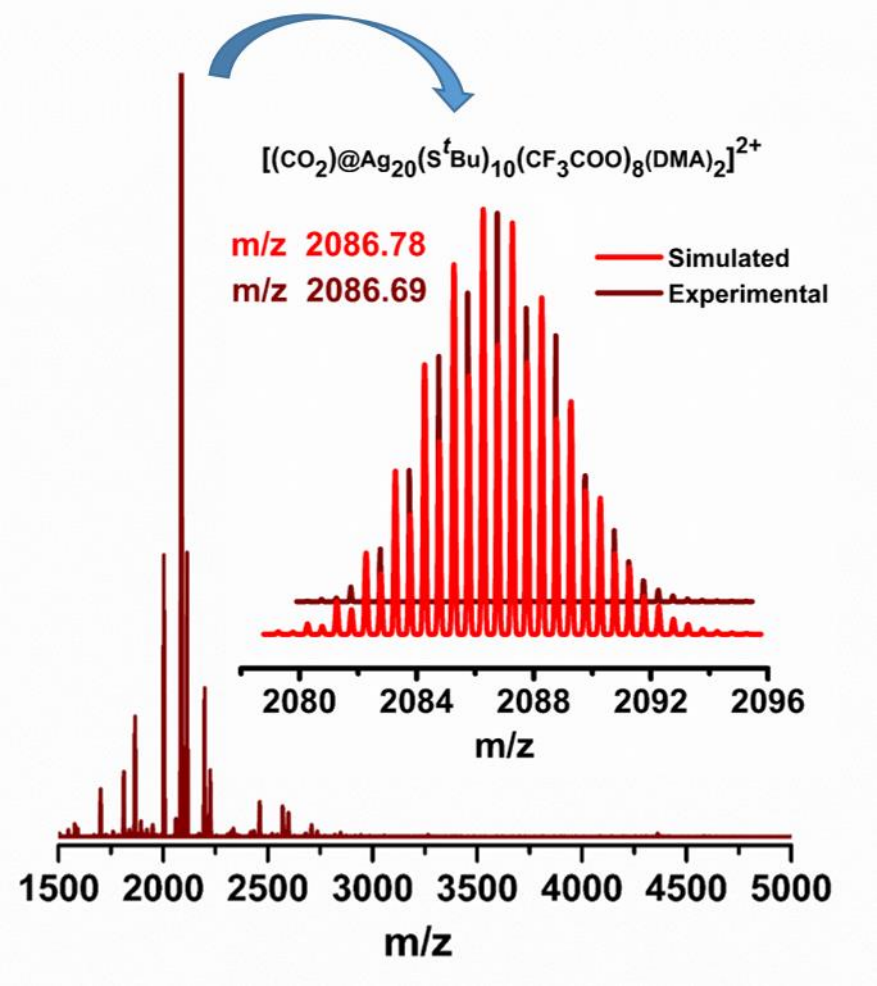

Fig. S5 The positive-mode ESI-MS spectrum of the intermediate.

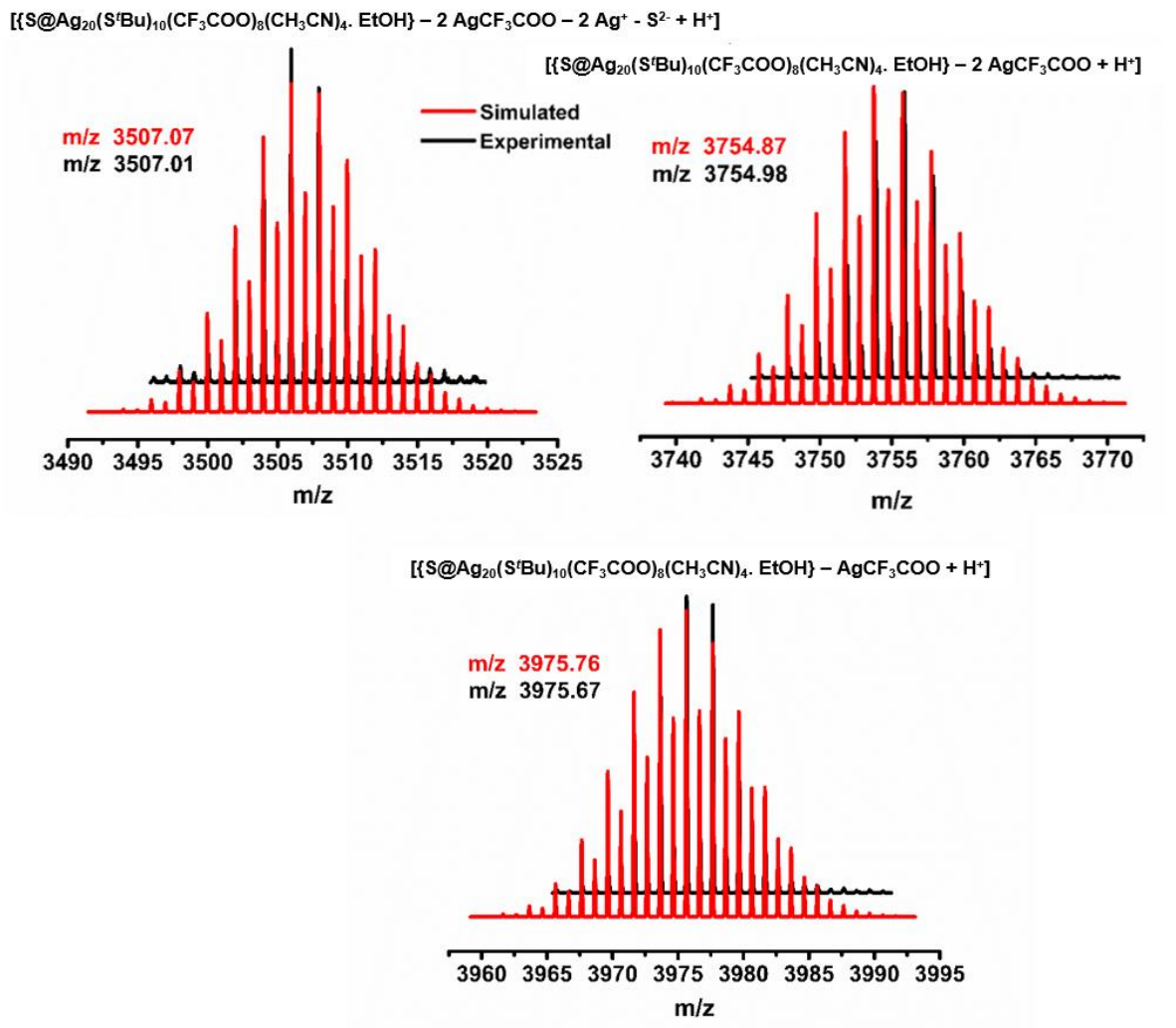

Fig. S6 The associated fragments of **NC 1** along with the peak experimental and simulated patterns.

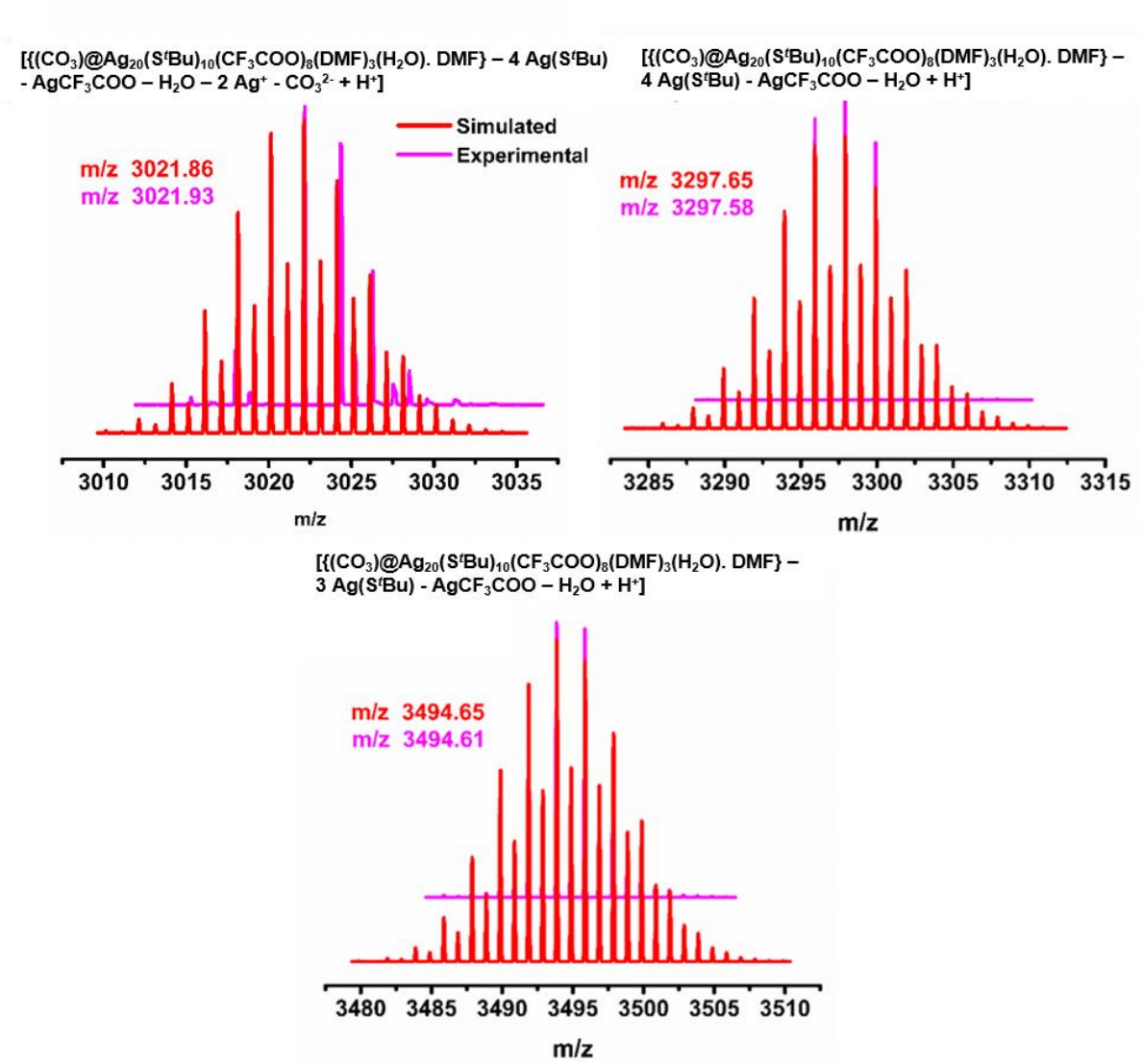

Fig. S7 The associated fragments of **NC 2** along with the peak experimental and simulated patterns.

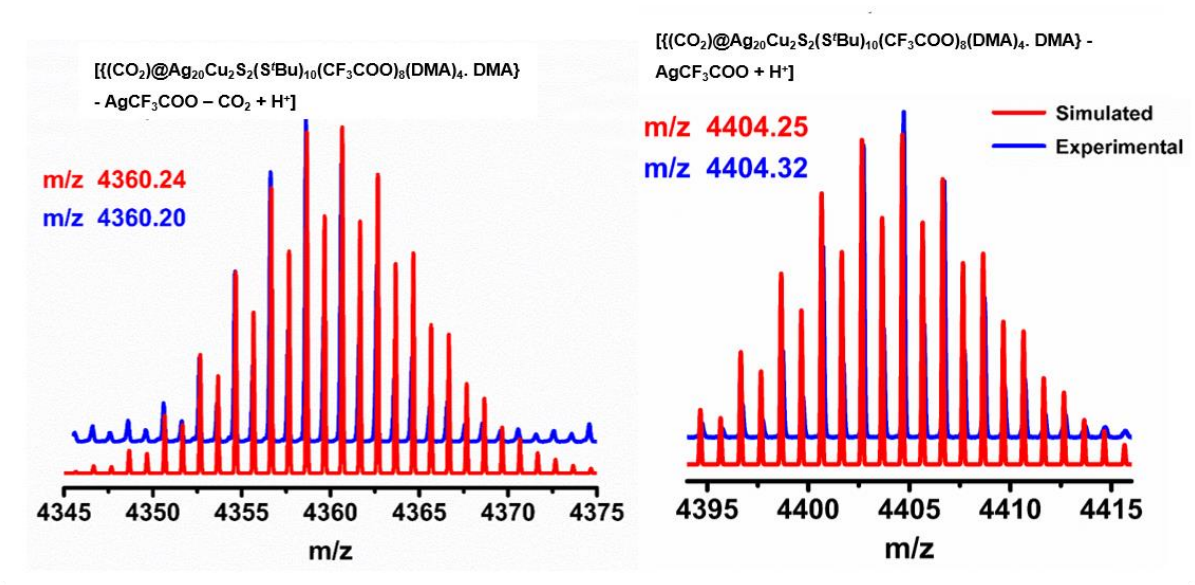

Fig. S8 The associated fragments of **NC 3** along with the peak experimental and simulated patterns.

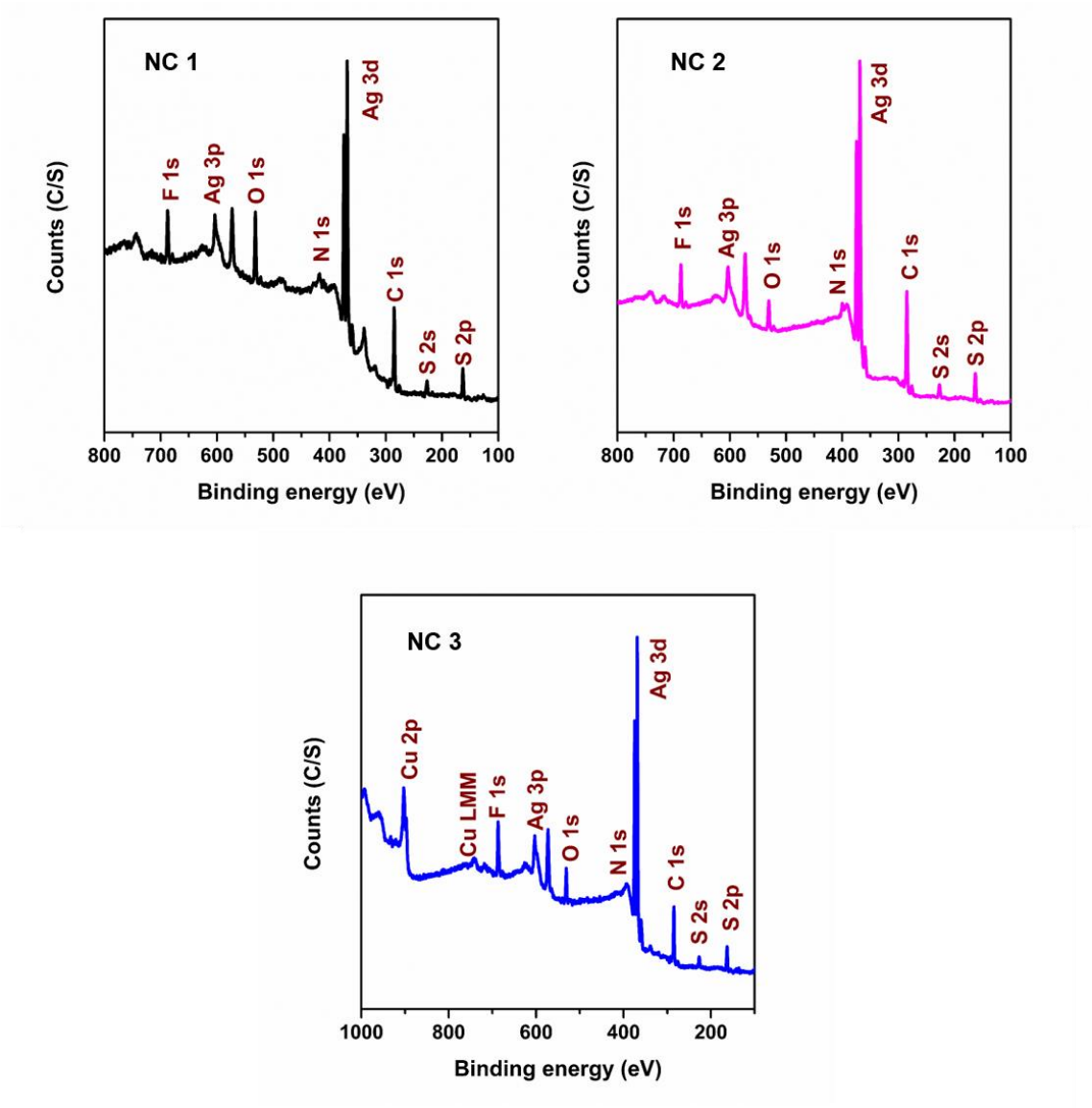

Fig. S9 The XPS survey spectra of three NCs.

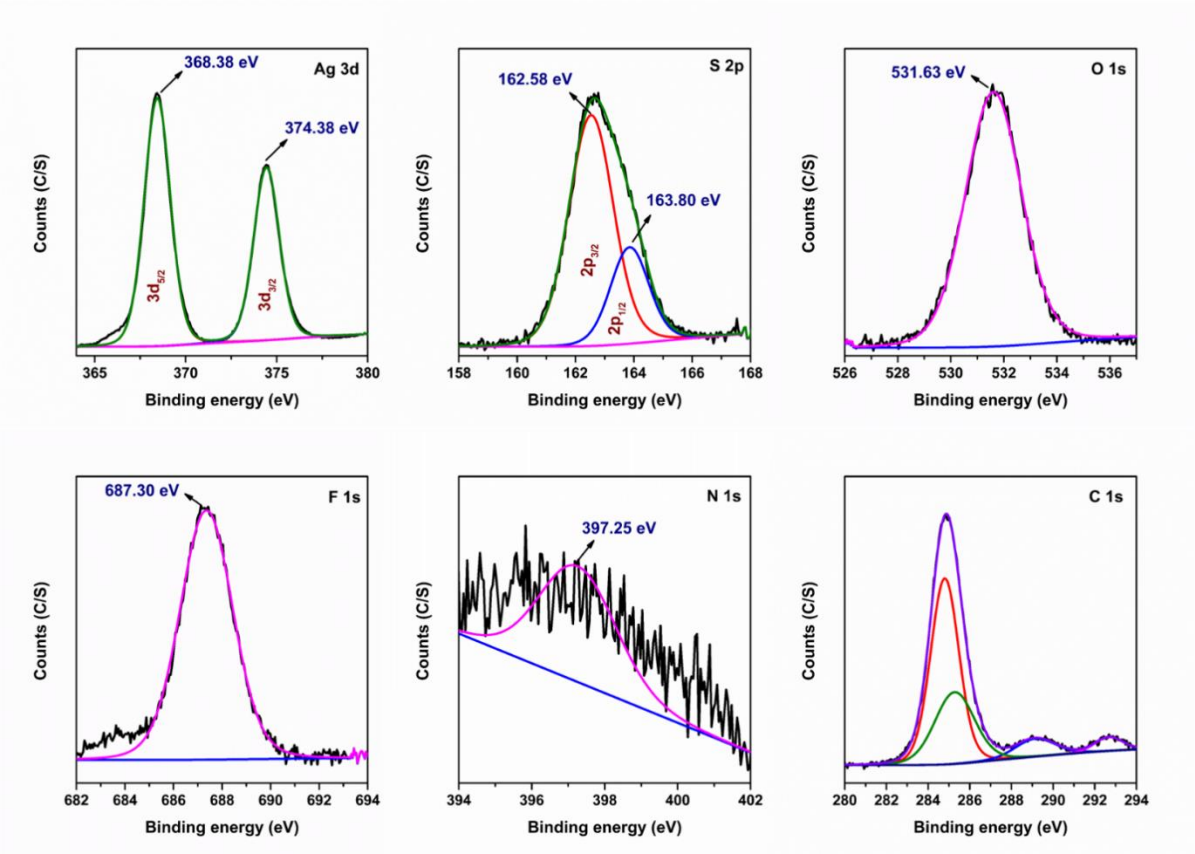

Fig. S10 The deconvoluted XPS spectra of the **NC 1**.

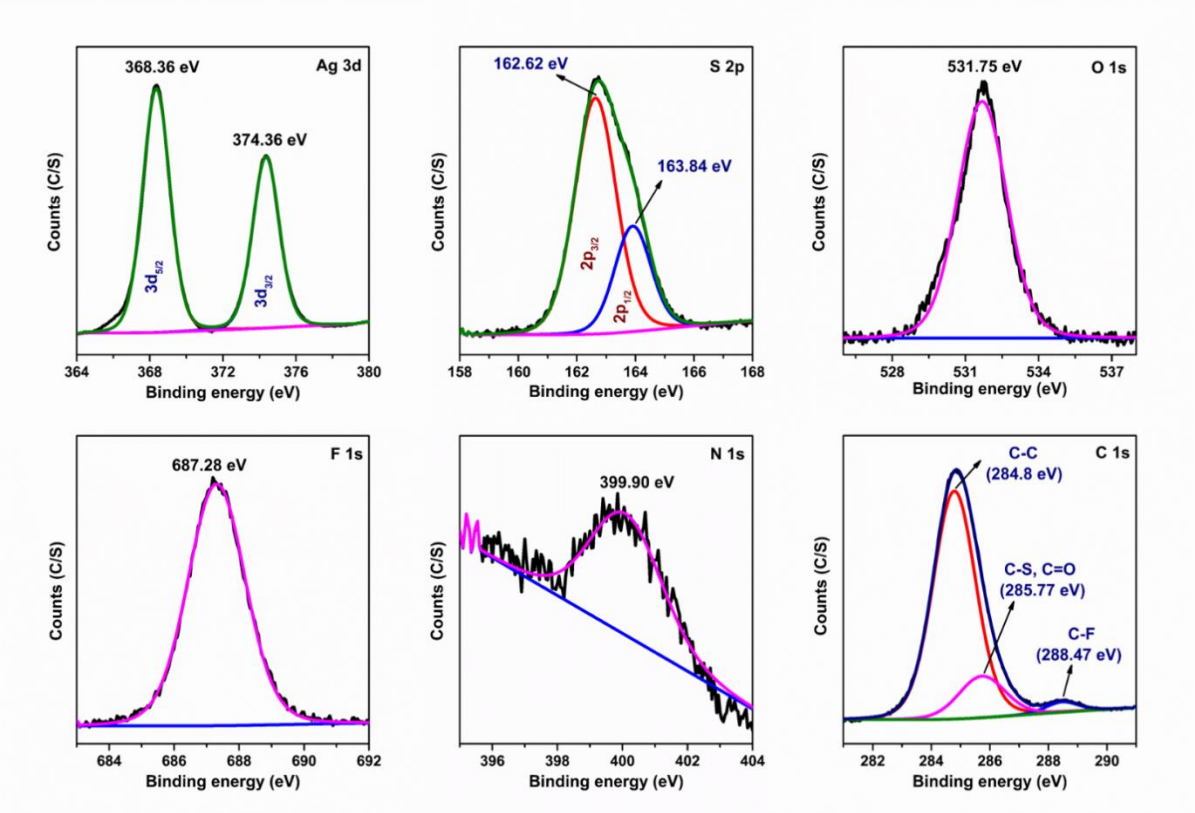

Fig. S11 The deconvoluted XPS spectra of the **NC 2**.

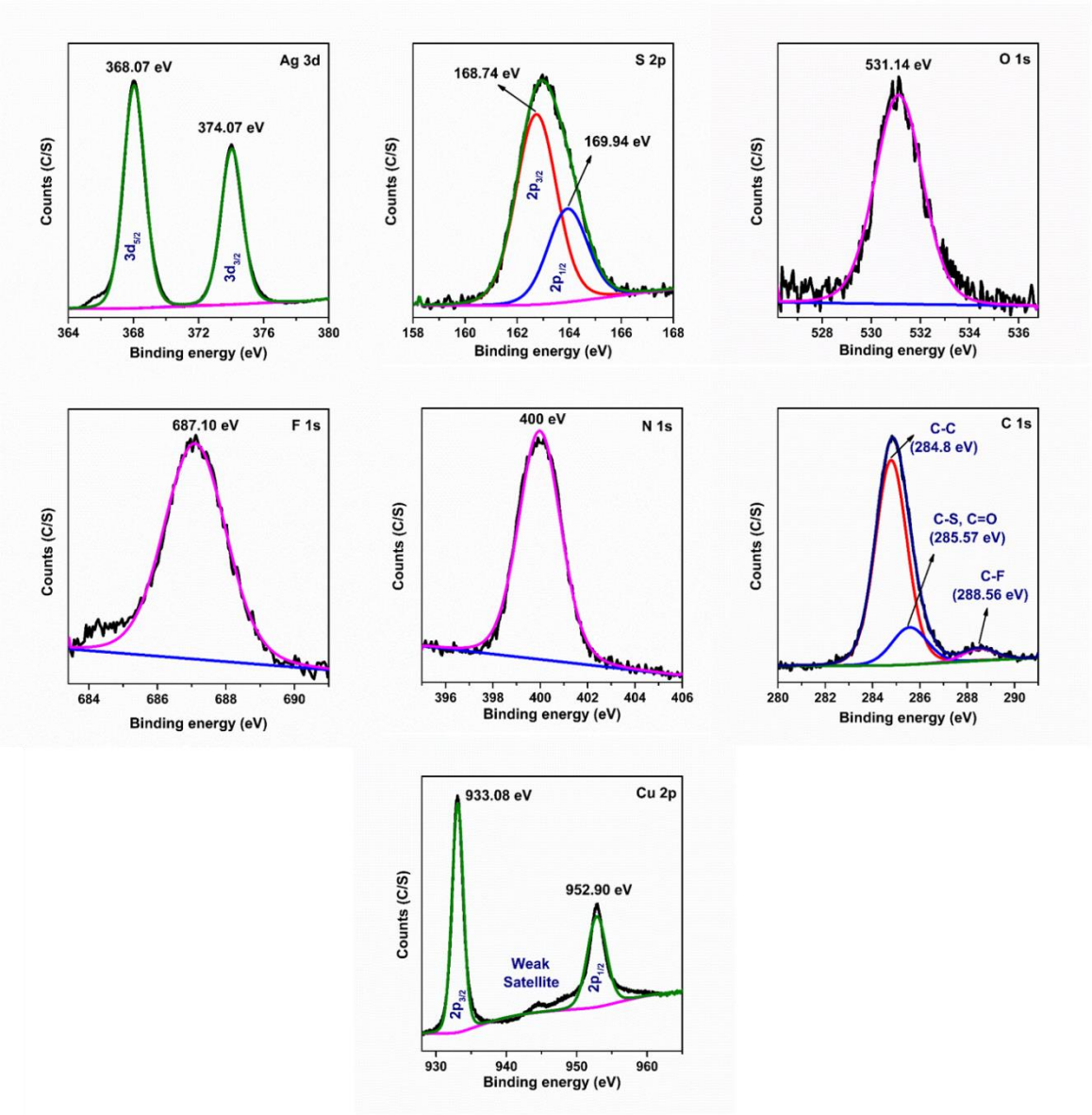

Fig. S12 The deconvoluted XPS spectra of the **NC 3**.

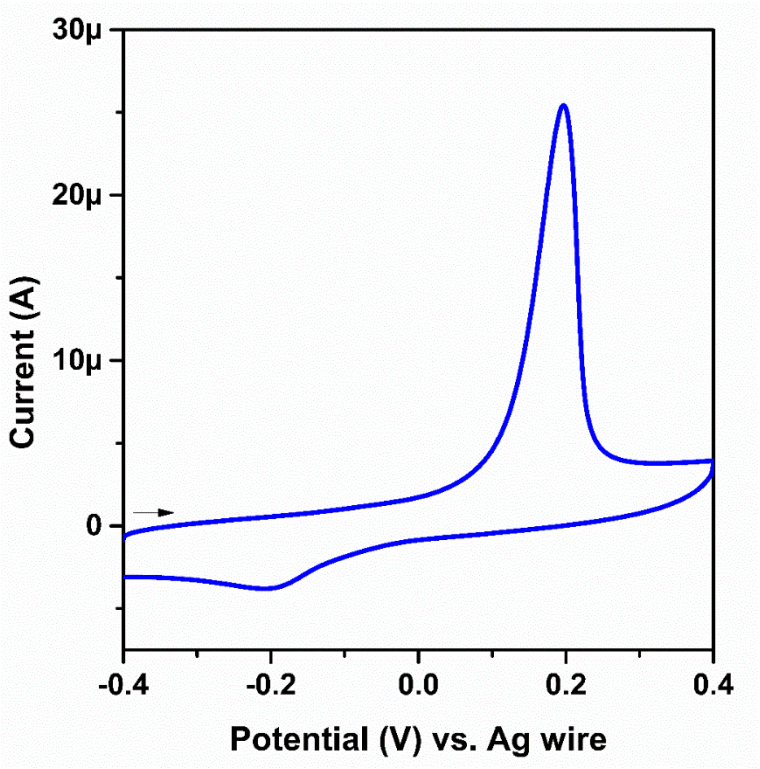

Fig. S13 Cyclic-voltammetry plot of **NC 3**.

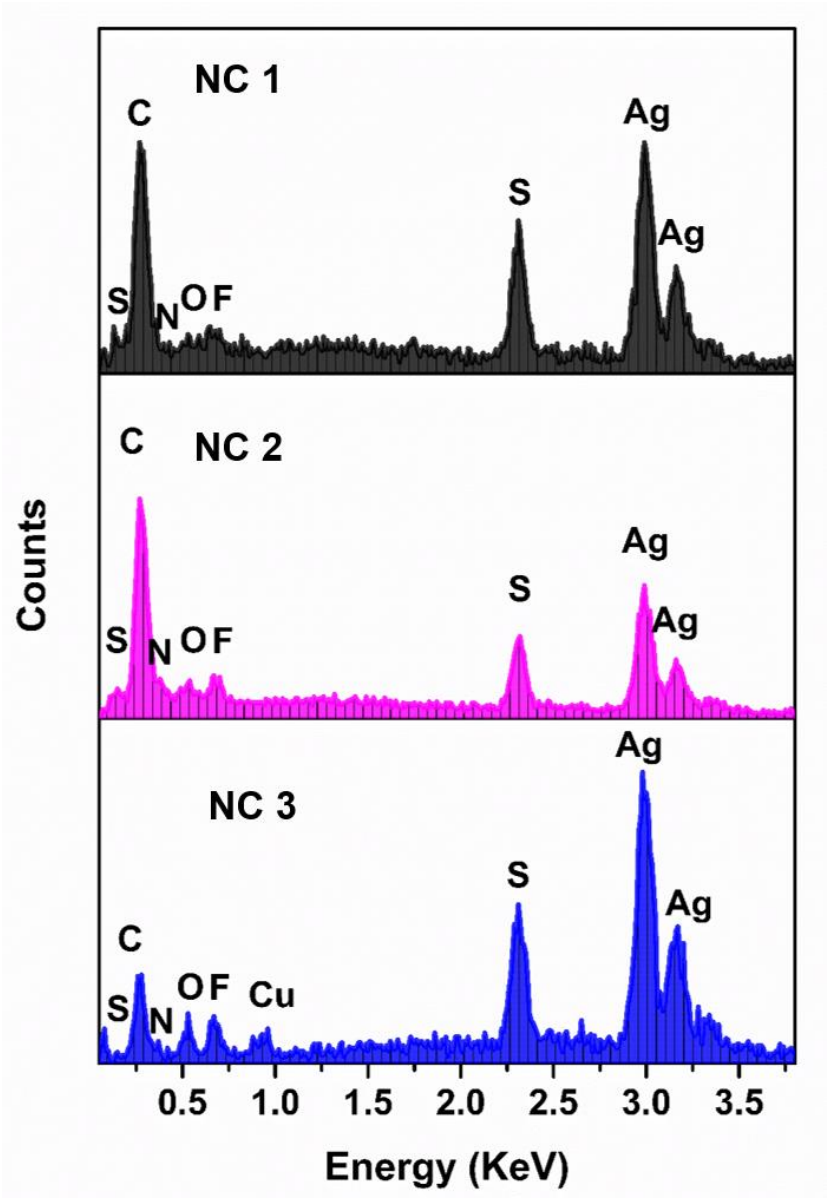

Fig. S14 EDS spectra of three NCs.

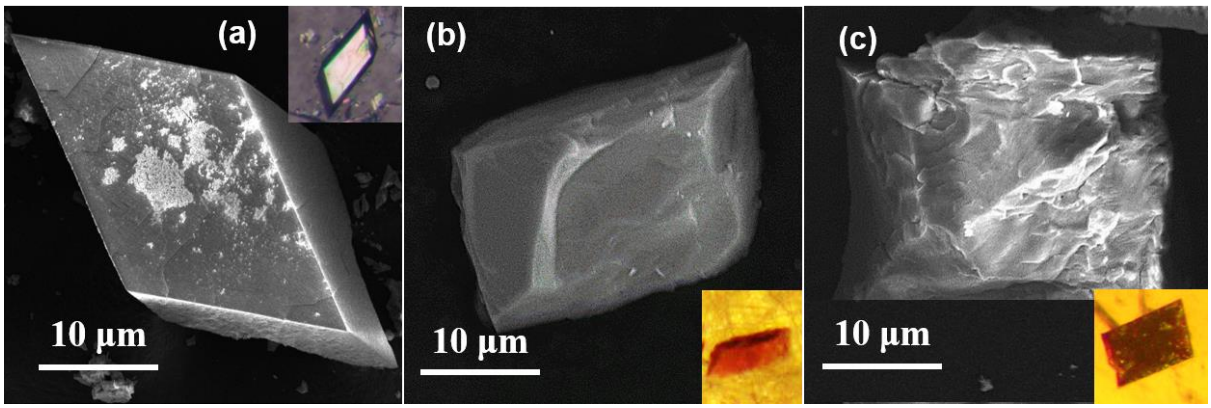

Fig. S15 SEM micrographs of (a) **NC 1**, (b) **NC 2**, (c) **NC 3** and the corresponding insets showing the optical-microscope image of each NC crystal.

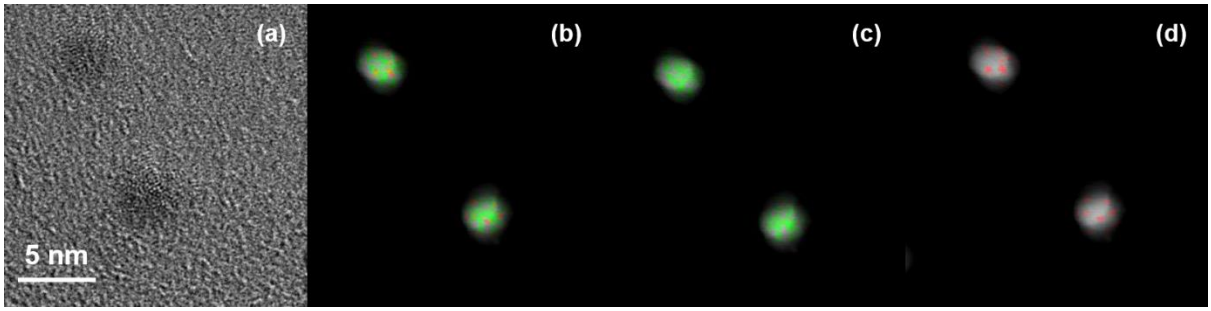

Fig. S16 (a) TEM image of the **NC 3** and elemental mapping of (b) both Ag and Cu, (c) only Ag and (d) only Cu.

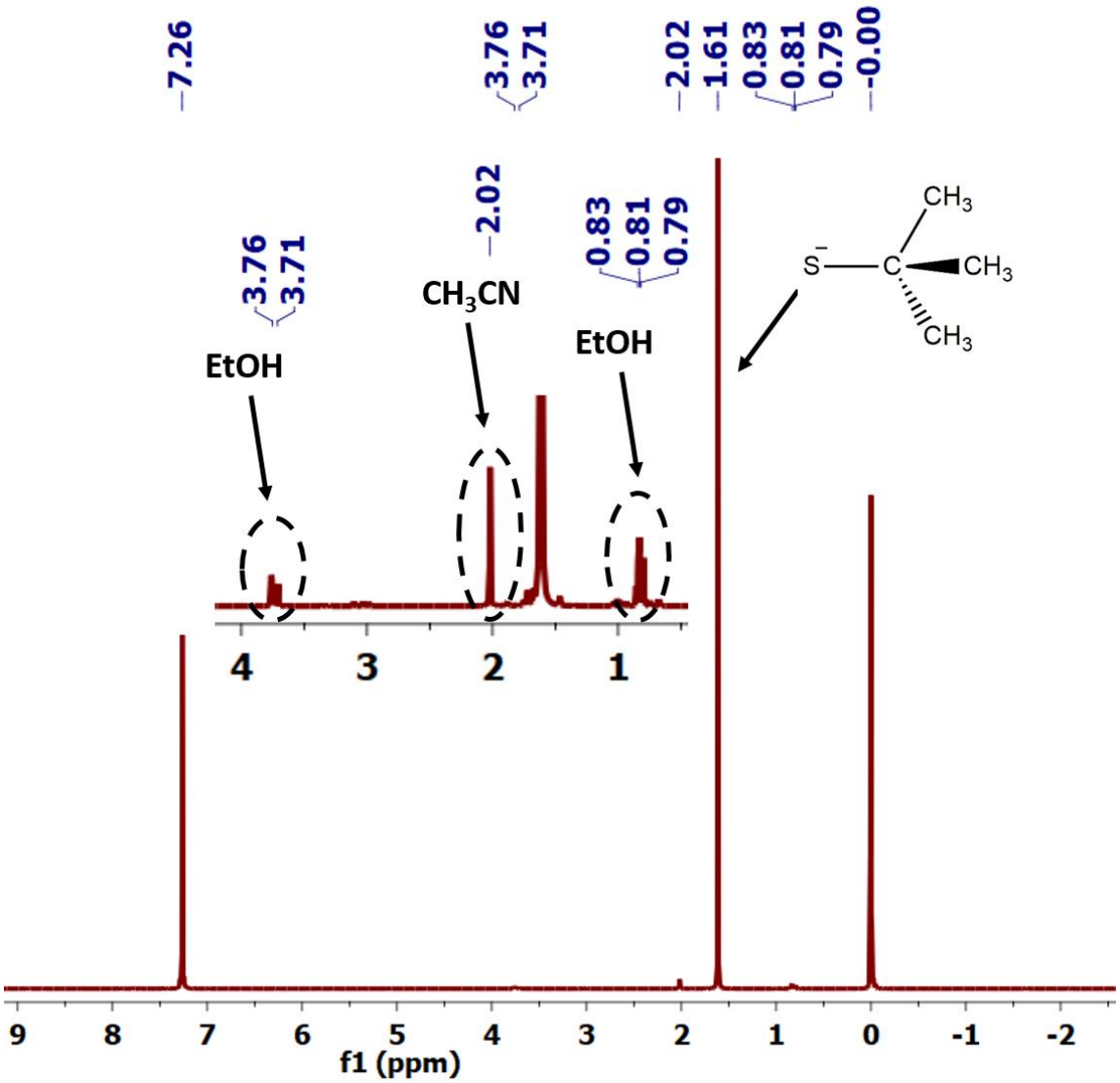

Fig. S17 The ^{1}H NMR of **NC 1** in $CDCl_3$.

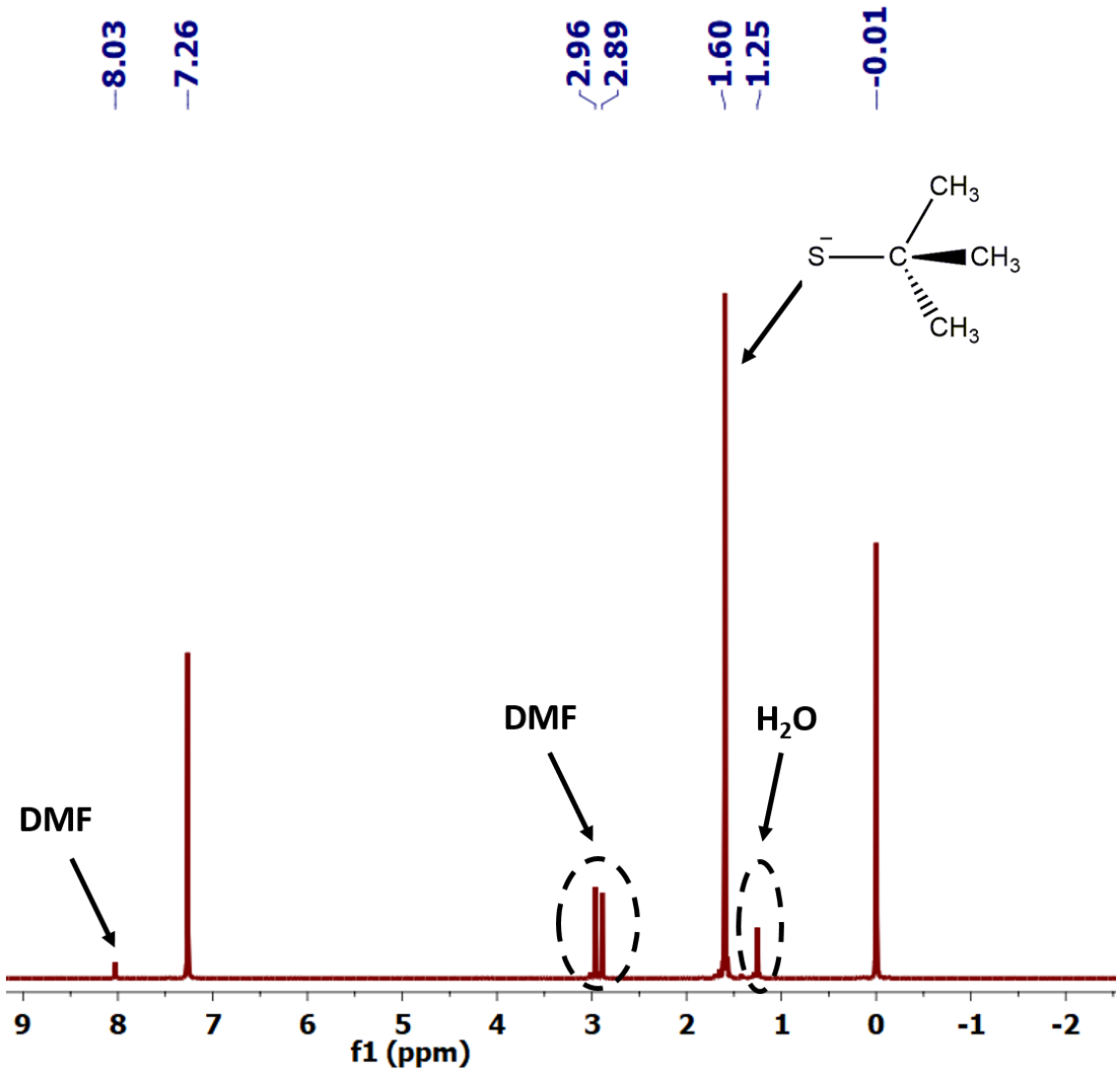

Fig. S18 The ^{1}H NMR of **NC 2** in $CDCl_3$.

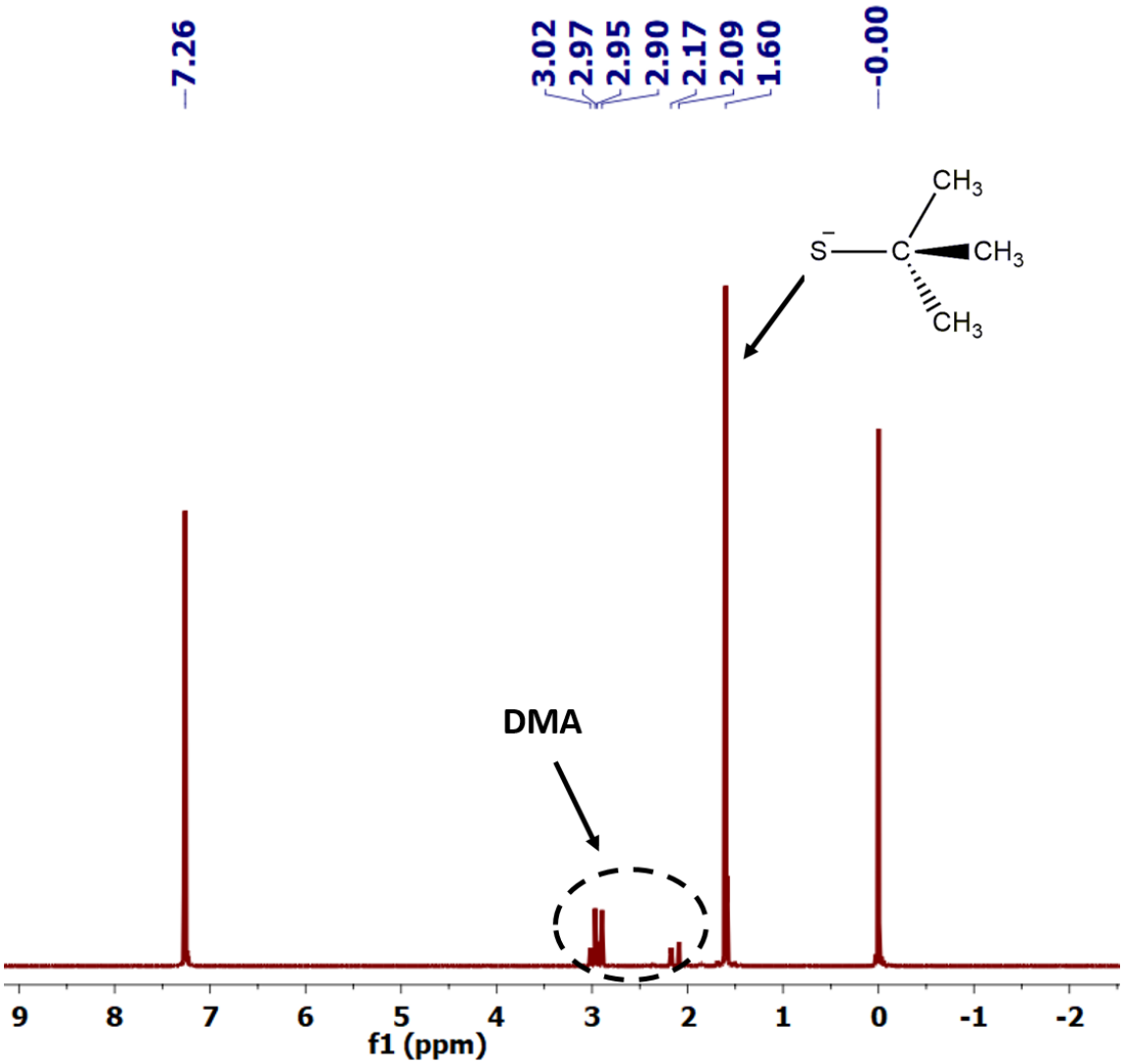

Fig. S19 The ^{1}H NMR of **NC 3** in $CDCl_3$.

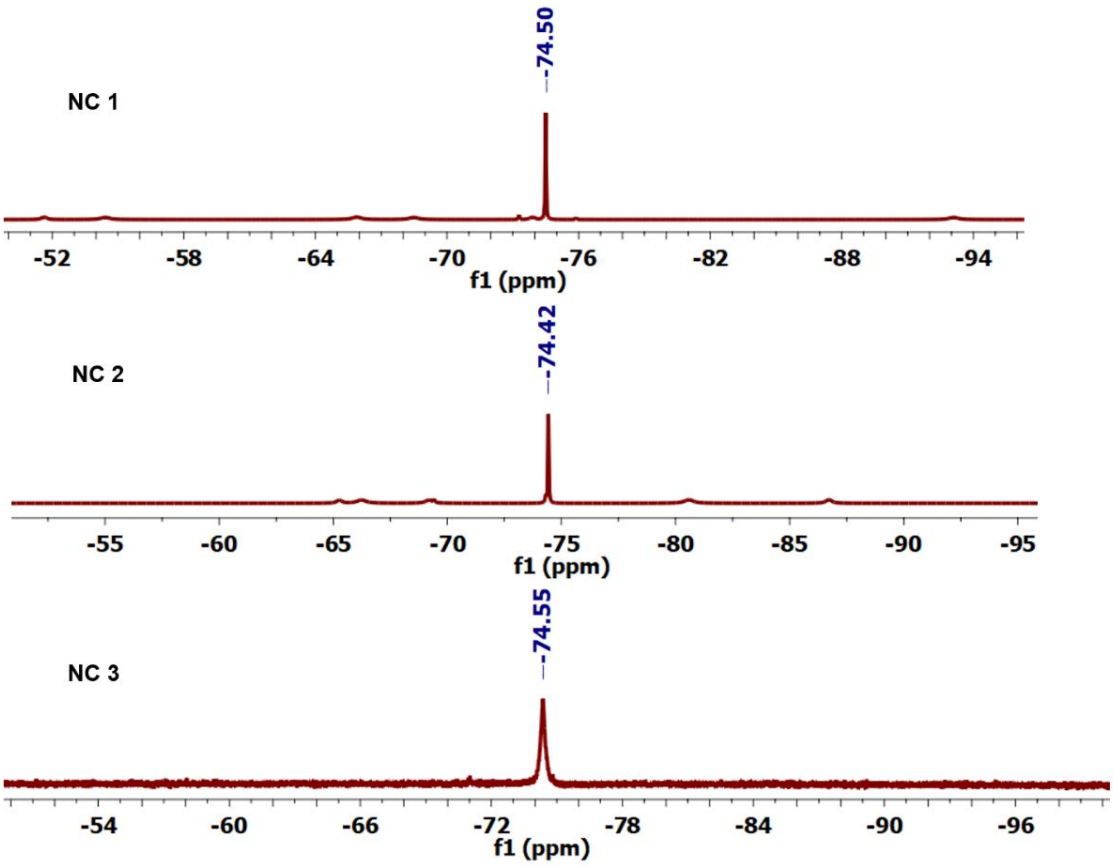

Fig. S20 The ^{19}F NMR of all NCs in $CDCl_3$.

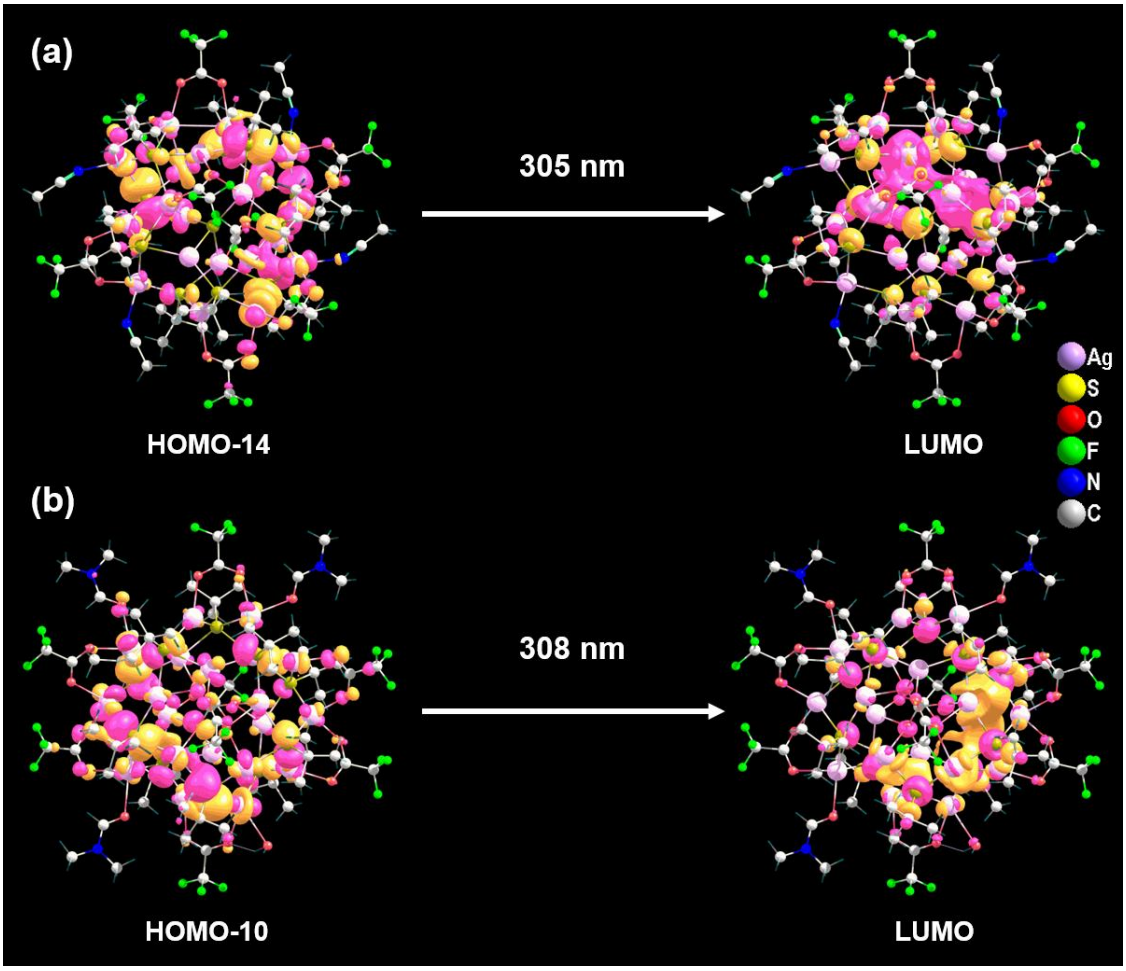

Fig. S21 The FMO of (a) **NC 1** and (b) **NC 2**.

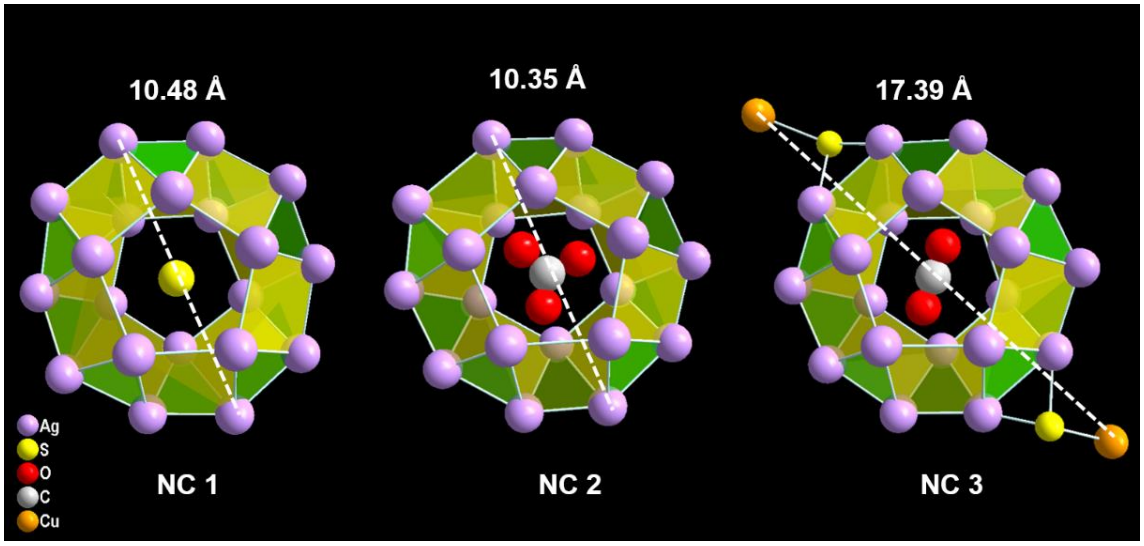

Fig. S22 Metal-to-metal distances in three NCs.

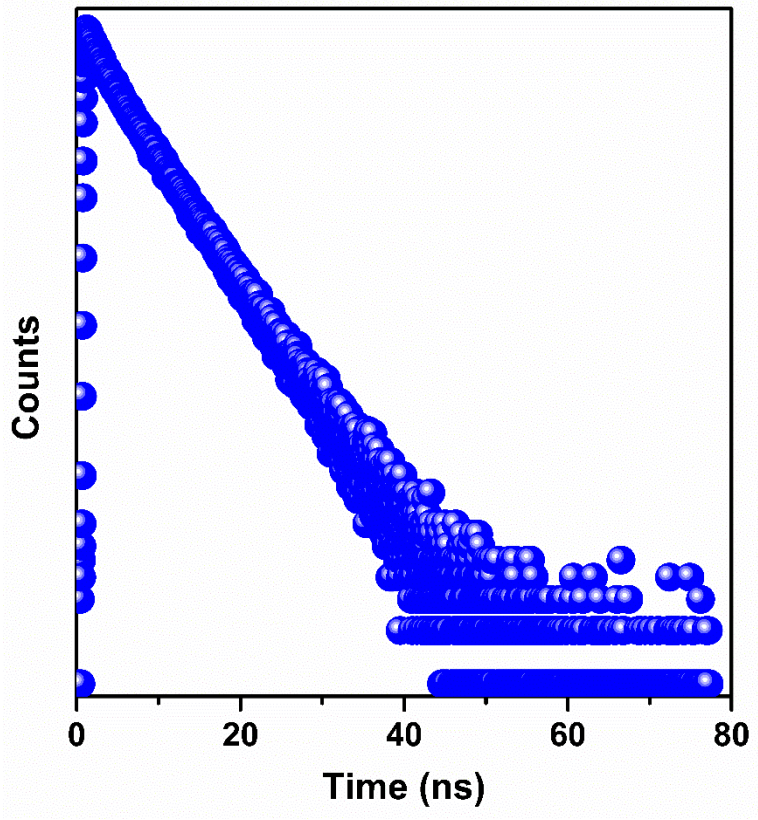

Fig. S23 Emission lifetime of **NC 3**.

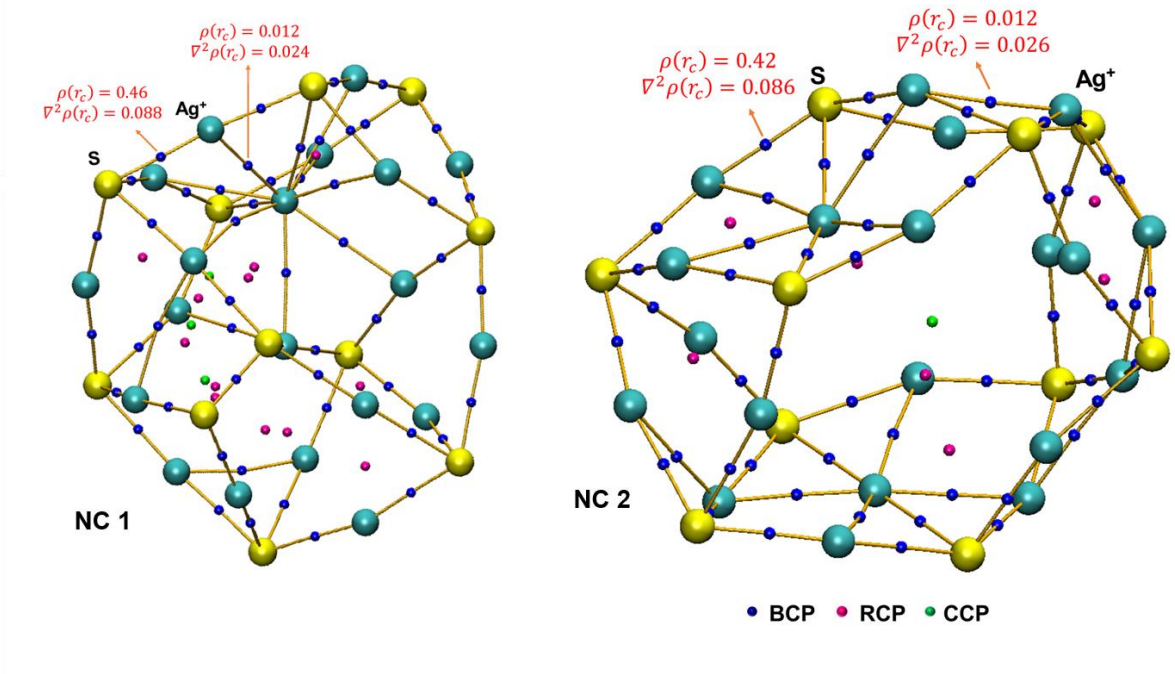

Fig. S24 QTAIM molecular plot of bond critical point (BCP), ring critical point (RCP) and cage critical point (CCP) of **NC 1** and **NC 2**. For clarity, we have removed the ligands.

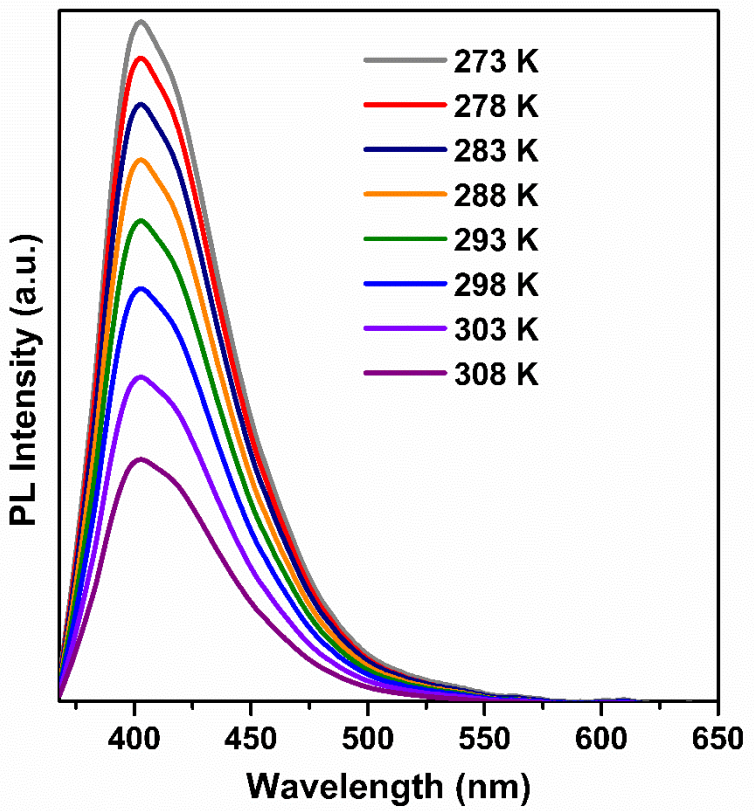

Fig. S25 Temperature-dependent PL emission of **NC 3**.

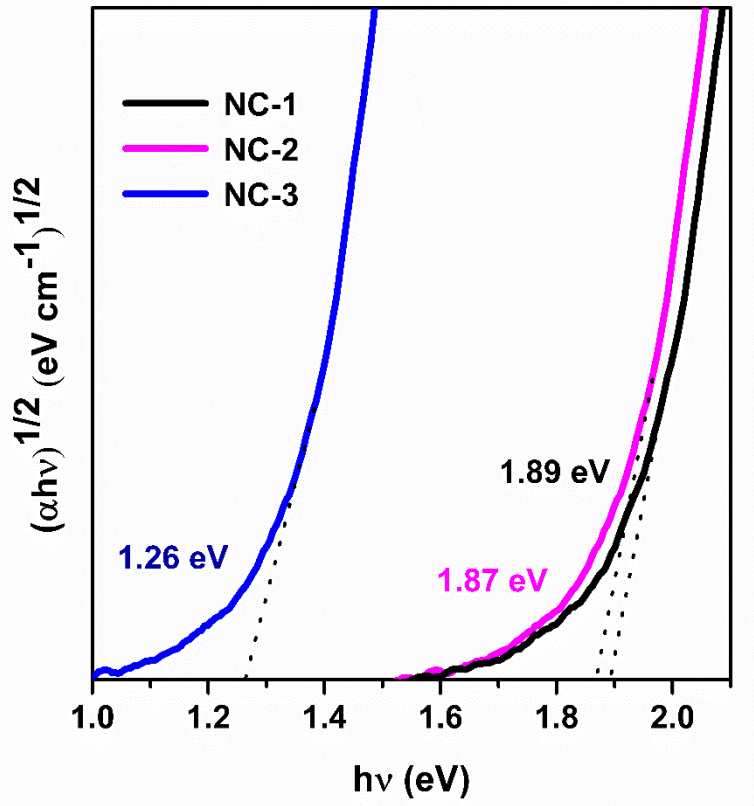

Fig. S26 Solid-state bandgap of each NC.

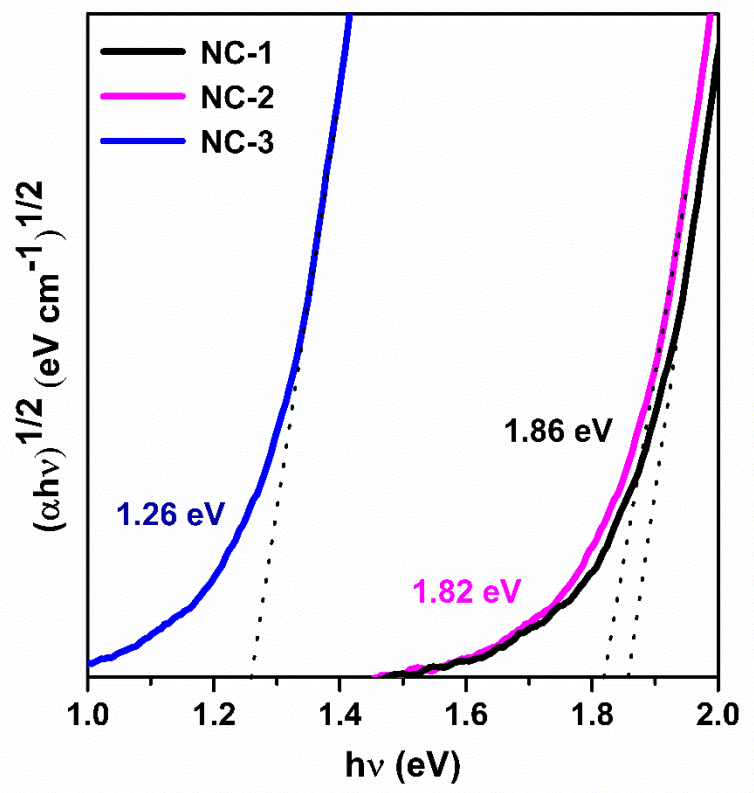

Fig. S27 Solid-state bandgap of each NC after 1 months of synthesis.

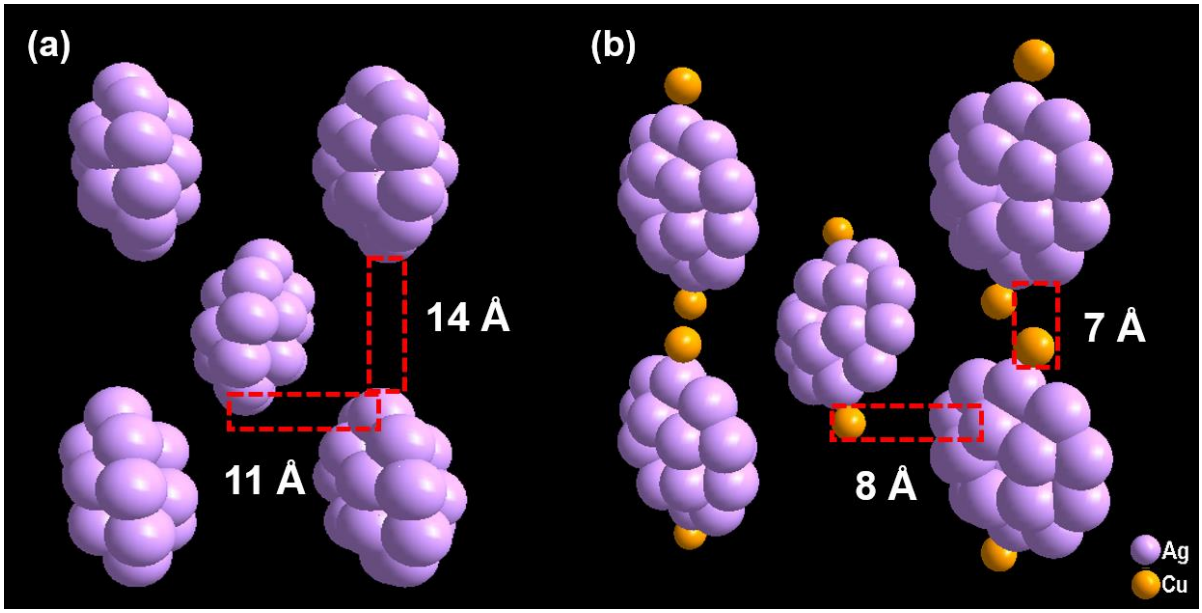

Fig. S28 Edge-to-edge and face-to-face distances of (a) **NC 1** and (b) **NC 3**.

References

S1. G. M. Sheldrick, *Acta Crystallogr. Sect. C: Struc. Chem.* 2015, **71**, 3-8.

S2. G. M. Sheldrick, *Acta Crystallogr., Sect. A: Found. Adv.* 2015, **71**, 3-8.

S3. L. J. Farrugia, *J. Appl. Crystallogr.* 2012**, 45**, 849-854.

S4. O. V. Dolomanov, L. J. Bourhis, R. J. Gildea, J. A. Howard, H. Puschmann, *J. Appl. Crystallogr.* 2009, **42**, 339-341.

S5. M. J. Frisch, G. W. Trucks, H. B. Schlegel, G. E. Scuseria, M. A. Robb, R. J. Cheeseman, G. Scalmani, V. Barone, B. Mennucci, G. A. Petersson, H. Nakatsuji, et al. Gaussian 09, Revision D.01; Gaussian, Inc.: Wallingford, CT, 2009.

S6. A. D. Becke, *J. Chem. Phys.* 1993, **98**, 5648-5652.

S7. A. D. McLean, G. S. Chandler, *J. Chem. Phys.* 1980, **72**, 5639 −5648.

S8. P. J. Hay, W. R. Wadt, *J. Chem. Phys.* 1985, **82**, 270 −283.

S9. P. J. Hay, W. R. Wadt, *J. Chem. Phys.* 1985, **82**, 299 −310.

S10. T. Lu, F. Chen, *J. Comput. Chem.* 2012, **33**, 580-592.

S11. T. Lu, F. Chen, *Acta Chim. Sinica*. 2011, **69**, 2393-2406.

S12. G. Kresse, J. Hafner, *Phys. Rev. B: Condens. Matter Mater. Phys.* 1994, **49**, 14251.

S13. J. P. Perdew, J. A. Chevary, S. H. Vosko, K. A. Jackson, M. R. Pederson, D. J. Singh, C. Fiolhais, *Phys. Rev. B: Condens. Matter Mater. Phys.* 1992, **46**, 6671.

S14. G. Kresse, D. Joubert, *Phys. Rev. B: Condens. Matter Mater. Phys.* 1999, **59**, 1758.